SAND2020-13411C

Integrated Fluid and Materials Modeling of Environmental Barrier Coatings

David Newsome[1], Rae Waxman[2], Andreas Hoffie[3]
CFD Research Corporation, Huntsville, Alabama, 35806, USA

Stewart Silling[4]
Sandia National Laboratories, Albuquerque, New Mexico, 87123, USA

Environmental Barrier Coatings (EBC) protect ceramic matrix composites from exposure to high temperature moisture present in turbine operation through its dense top coat. However, moisture is able to diffuse and oxidize the Si bond coat to form SiO_2, where incorporation of O causes swelling and tension. At sufficient swelling the EBC will fail due to increase damage such as delamination. A multiscale simulation framework is developed to link operating conditions of a high-performance turbine to the failure modes of the EBC. CFD simulations of the E3 turbine were performed and compared to prior literature data to demonstrate the fidelity of the Loci/CHEM software to determine the flow conditions on the turbine blade surface. Boundary condition data of pressure and heat flux were then determined with the CFD simulations, providing the temperature at the bond coat. Peridynamics was used to model the microscale TGO growth. A swelling model that links moisture concentration to the stress at the TGO due to the volume increase from oxidation was demonstrated, coupling moisture transport to localized stress and directly observing TGO growth and the corresponding damage. This framework is generalized and can be adapted to a range of EBC microstructures and operating conditions.

I. Nomenclature

m	=	Mach number to represent velocity
p	=	pressure
v	=	velocity

II. Introduction

The development and use of advanced materials in next-generation gas turbine engines is a key feature of the NASA materials development roadmap, with the goal of increasing the operating efficiency by running at higher temperatures [1]. In order to achieve this goal, ceramic matrix composites (CMC) are under development as alternative materials to superalloys for engine components. The safe and reliable use of the Si-based materials in the hot sections of gas turbine engines is critically reliant upon the performance and integrity of the environmental barrier coating (EBC) system. The durability and, correspondingly, the viability of parts fabricated using ceramics for use in gas turbine applications depend on the long-term performance of the EBC. It is prohibitive in time and cost to replicate the range of service conditions in controlled experiments, and, likewise, there is uncertainty in correlating experimental conditions to those in service. CFD Research is developing a physics-based simulation workflow and multiscale model of an EBC system interacting with the flow environment, to provide a means to gain better understanding of the dynamic processes that effect EBC durability and performance under service conditions. The

[1] Principal Engineer; Energy, Materials, and Propulsion Division; AIAA Member.
[2] Research Engineer; Energy, Materials, and Propulsion Division.
[3] Research Engineer, Aerospace and Defense Solutions, AIAA Member.
[4] Distinguished Member of the Technical Staff; Computational Multiscale Department; AIAA Member.

modeling procedure uses computational fluid dynamics (CFD) to establish the conditions and species concentrations at the part surface.

III. CFD of Turbine Blade

CFD simulations of turbine blades have been performed with the Loci/Chem code [2] to assess the pressure and temperature distribution on the surface due to surrounding flow, providing a direct link of environmental conditions to the microstructure. The mesh of the turbine blade shape is based on the Energy Efficient Engine (E3) blade developed at NASA [3-7], as presented in Fig. 1, which shows the E3 turbine and a rotor blades and stator vanes of interest for EBC deposition.

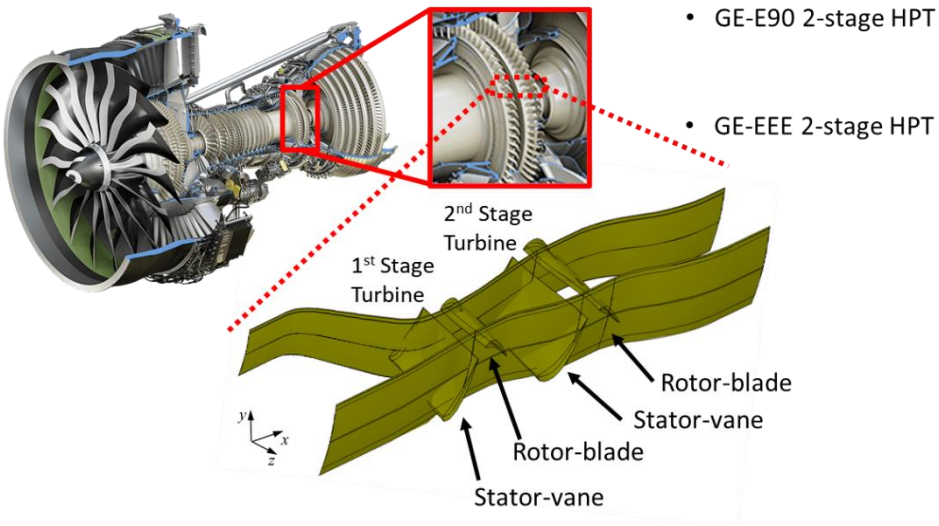

Fig 1 E3 turbine and blades modeled in CFD [3-7].

Figure 2 shows the detailed procedure of determining the 2D mesh of a rotor blade. Starting from the provided E3 geometry, the rotor-blade of the first stage is isolated and a slice taken at mid-span. The mesh is then created along this surface and some distance out. The definitions for the boundary conditions are included in Fig. 3 used for the CFD simulation.

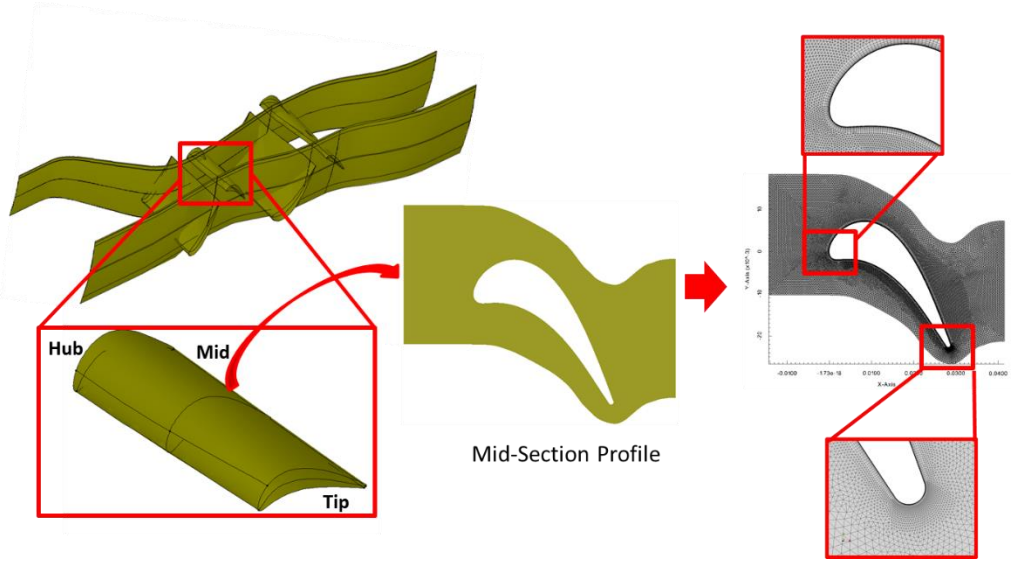

Fig 2 Mid-section profile of rotor blade along with CFD mesh.

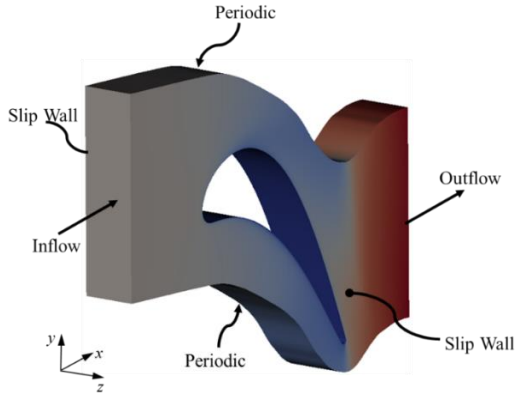

Fig 3 Boundary condition definitions of a blade.

Steady and unsteady analysis is being conducted on this 2D mesh, as it was found that the averaged unsteady wake has an effect on the heat transfer distribution [7]. Typical quantities for comparison are pressure and heat flux. As the CFD simulations assess the surface conditions on the turbine blade, the pressure, temperature, and species concentrations will be determined and linked back to the peridynamic (PD) microstructural simulations, as the transport rates will increase with response to higher temperature, pressure and moisture, creating a top-down multi-scale methodology. Figure 4 presents the velocity field, pressure field, and Mach field along the blade surface and in the surrounding region, along with the Mach field in a blade cascade. The pressure and heat flux at the blade surface are also determined in the CFD simulation, presented in Fig. 5, as a function of the normalized surface position, (negative position is bottom of blade, positive position is top of blade), and directly provide the microscale boundary conditions that affect TGO growth in the EBC. The values vary significantly, with peak values at the stagnation point (Relative Distance = 0) and fluctuations at the tail end.

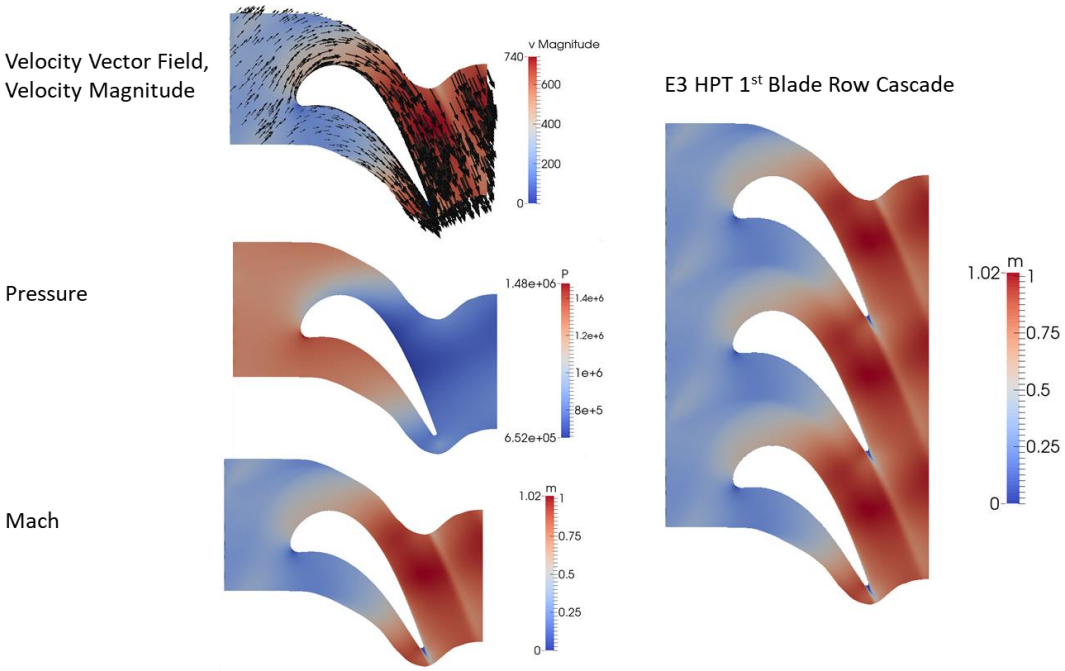

Fig 4 Velocity, Pressure and Mach fields surrounding the blade (left); flow field in the blade row cascade (right).

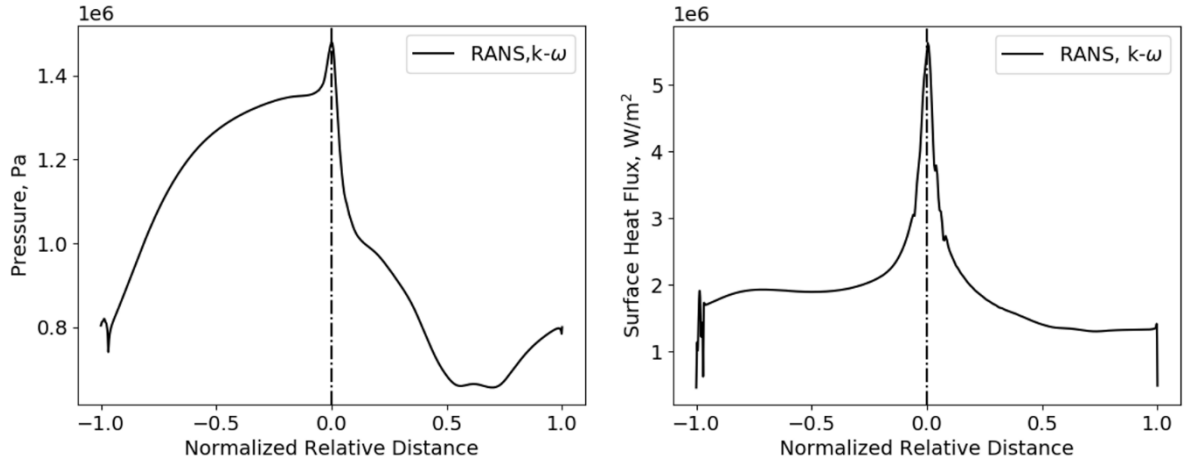

Fig 5 Pressure and heat flux on the turbine blade surface, which provides microscale boundary condition data.

IV. Virtual EBC Microstructure

The response of the coating materials is modeled at the microscale where each constituent phase of the coating system is discretely resolved. The micromechanics model is based on peridynamics, a theory of continuum mechanics that is well suited to model damage in brittle ceramic materials [8]. The virtual microstructure of a two-layer EBC, consisting of a splat grain top coat and equiaxial bond coat, was developed using the DREAM.3D software and custom scripts that combined the individual synthetic microstructures [9]. Figure 6 shows the virtual microstructure of EBC with splat grain top coat and equiaxial bond coat. The meshless peridynamics code EMU [10] was adapted to include mass transport in cracks and to model a multi-grain description of the microstructure. The microstructures are based upon experimental micrographs that resolve the grain structure and are used to guide the development of virtual microstructure grids.

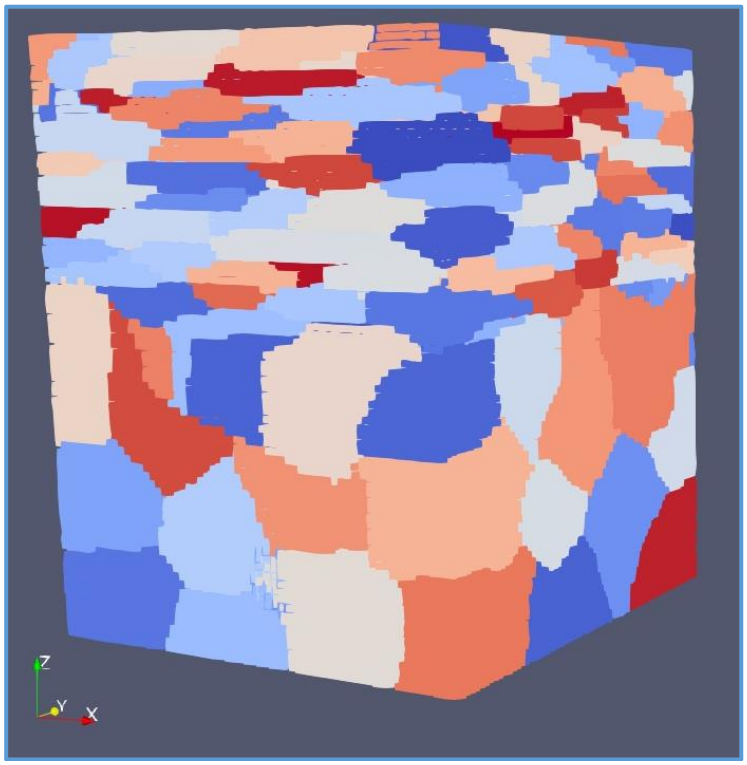

Fig 6 Virtual microstructure of an EBC with splat grain top coat and equiaxial bond coat.

V. Coupled Transport and Moisture Swelling

A swelling model is being applied to assess strain due to an increase in volume due to thermally grown oxide (TGO) at the interface of the top coat and bond coat within a PD framework [10]. As moisture diffuses through the cracks and material, it reacts with the bond coat material, incorporating into the framework of the crystal to cause a localized swelling and internal strain. Transport of moisture occurs over a longer time scale compared to the internal swelling but must be coupled to the TGO growth rate using an accelerated transport rate to make the simulation feasible with the explicit solver that EMU uses for mechanical response and transport. As moisture accumulates in the material nodes, the swelling increases, with the concentration of moisture predicted by the transport rates provided as input to the swelling model. The subsequent enlargement of the TGO will displace nodes at the interface, causing buckling and cracking between the top coat and bond coat. To relate the accelerated moisture transport to physical time scales, the oxide thickness is calibrated using experimental TGO growth curves that measure TGO thickness to oxidation time.

As internal damage increases, more cracks form and accelerated moisture transport occurs. The coupled cracking and transport set-up is featured in Fig. 7, showing a typical equiaxial microstructure, and Fig. 8, showing representative snapshots of increasing crack growth and moisture concentration at two times during the microscale simulation. At 6,000 time steps, extensive damage is present, but the cracks do not yet form a network that provides continuous pathways for transport between the upper and lower surfaces. So, at 6,000 time steps, the net flux is low. At 22,000 time steps, there are many such complete pathways, and the net flux is much higher. The increased cracking is defined as increased number of broken material bonds, so that the local permeability in the transport model increases with node damage.

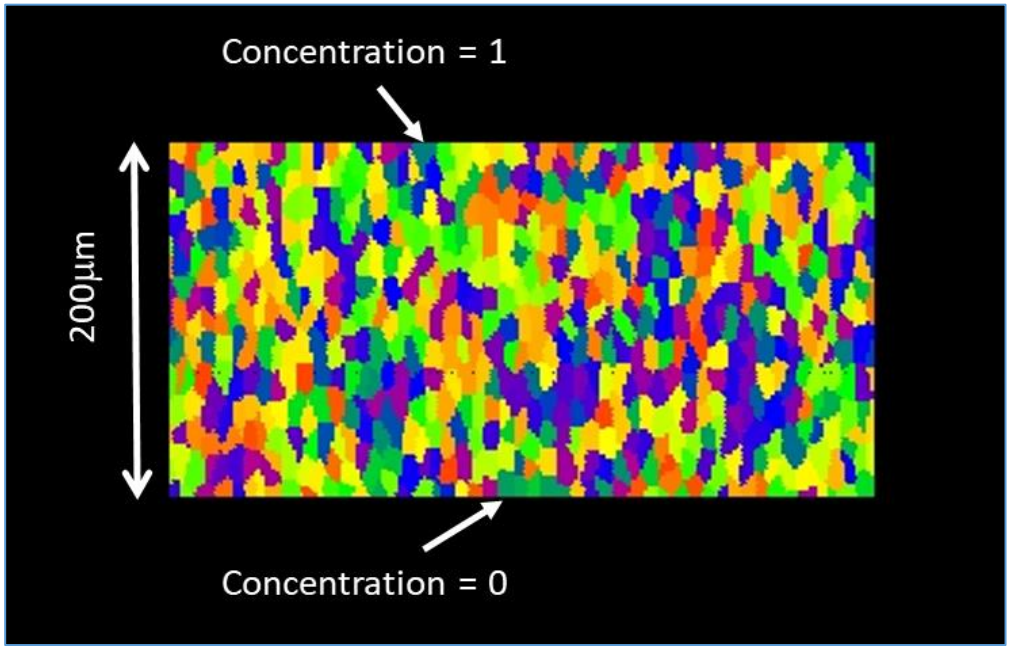

Fig 7 Microstructure of equiaxial grains for testing the coupled transport-crack simulation.

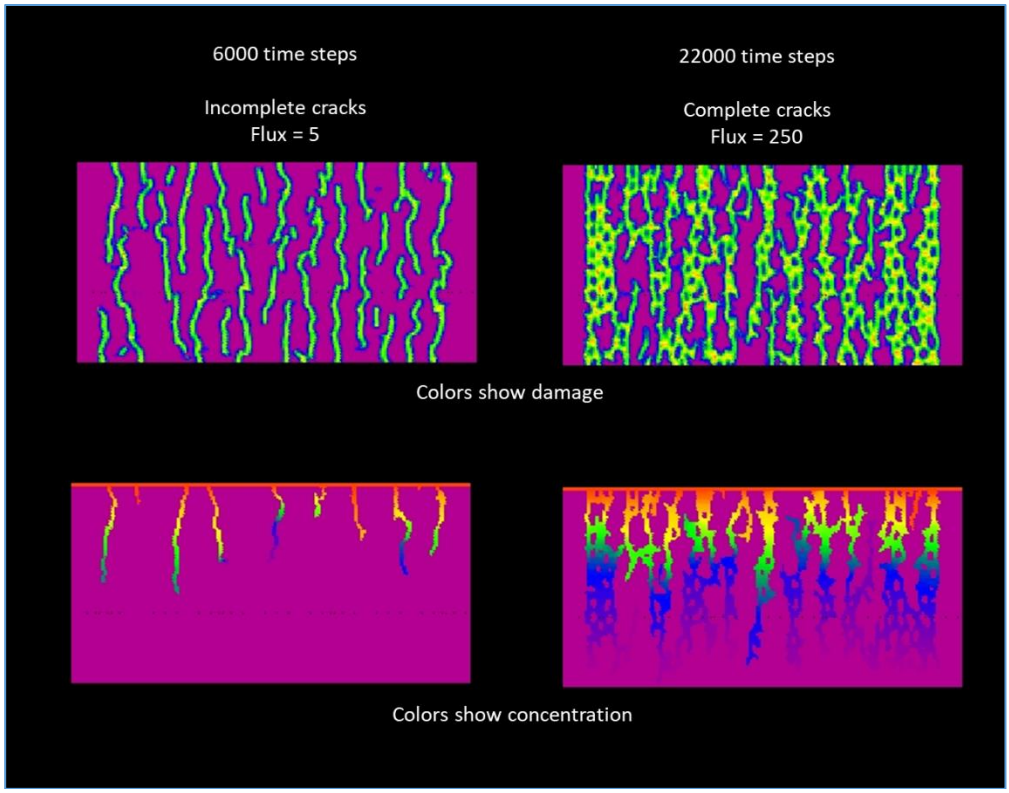

Fig 8 Damage from crack growth and concentration of moisture in equiaxial microstructure.

As moisture permeates through the BSAS top coat and Mullite + BSAS bond coat and reaches the Silicon bond coat, a thermally grown oxide (TGO) layer forms due to oxidation of Silicon (Si) into Silica (SiO_2). To model TGO formation and growth, an existing state-based PD model is being modified to capture linear elastic behavior with diffusion and moisture swelling. As material points absorb moisture and "oxidize", material properties (both elastic properties and damage criteria) will shift as well, with 0% moisture concentration corresponding to Silicon, and 100% moisture concentration corresponding to Silica. Concentrations between 0 and 100% will have transition properties between the two materials. The CME in Silicon can be adjusted to match experimental observations of TGO growth and swelling, which indicate volumetric changes on the order of 2:1 for incorporating oxygen as SiO_2:Si.

Diffusion in all materials is being modeled using a nonlocal form of Fick's Law. To accompany the diffusion subroutine, a concentration boundary condition was written and implemented. In the non-Silicon materials, the coefficient of moisture expansion (CME) is set to zero so no swelling occurs. In the Silicon nodes, the CME is nonzero and causes swelling according to the equation Stretch = CME x delta_moisture, where delta_moisture is the difference between current moisture concentration and a baseline (typically zero). This CME can also be updated based on concentration, the same way a coefficient of thermal expansion changes with temperature.

Two material layers were modeled in the simulation, as presented in Fig. 9. The right half of the grid had a CME of 0 while the left half had a CME of 10^{-10}. The concentration and displacement boundary conditions remained the same. With a CME of zero, the right side of the grid does not experience moisture swelling. Once the concentration gradient spreads and the left side of the grid has non-zero concentration values, swelling begins to occur at the interface. This can be seen in the concentration and displacement time progression in Fig. 9.

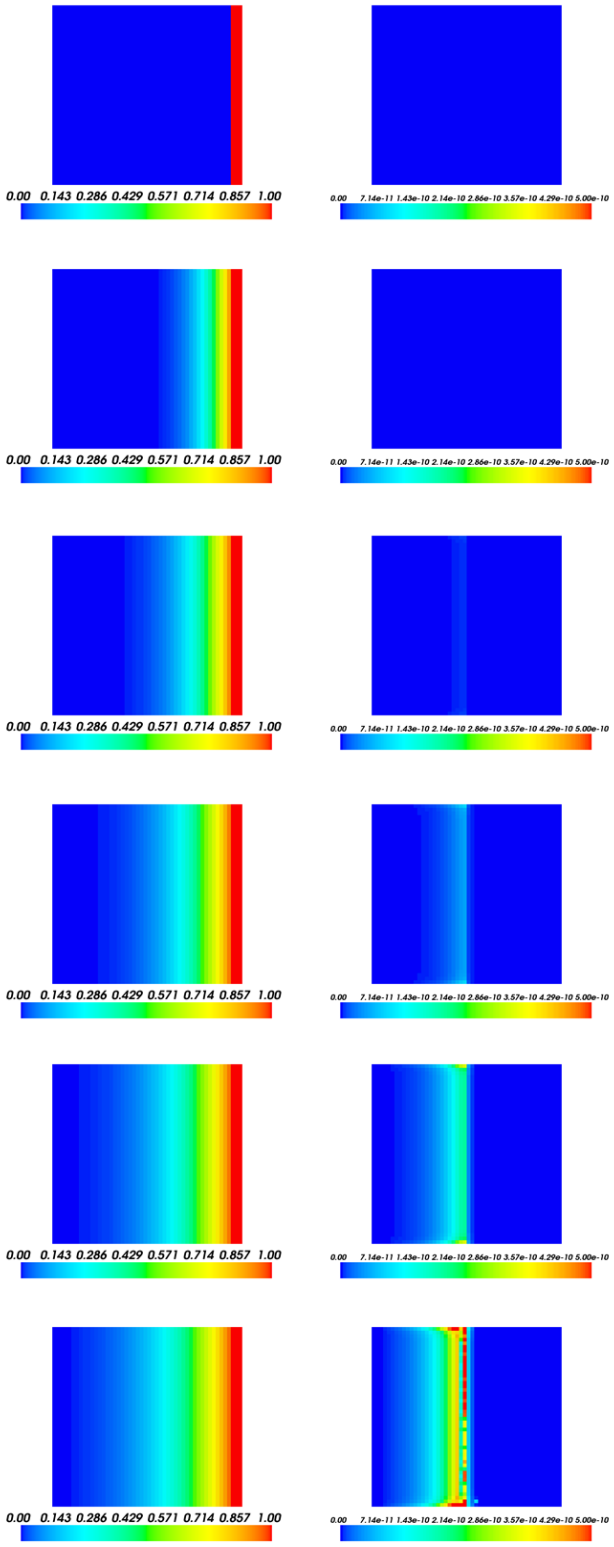

Fig 9 Concentration (left) and displacement magnitude (right) over time, two material moisture swelling case study. The swelling displacement occurs in the mid-point, representing creation of TGO.

VI. Conclusion

TGO is a significant failure mode in EBCs, and modeling tools are necessary to further understand the multiscale phenomena. CFD simulations of the turbulent flow in the E3 turbine were performed to determine the microscale boundary conditions, such as pressure and heat flux. The information is then being provided to the PD simulations of the TGO growth. PD uses a moisture expansion model of stress coupled to Fickian transport, which was demonstrated for a two-material grid, representing the top coat and bond coat initially, along with displacement from the creation of TGO. This modeling framework is currently being extended to include more realistic microstructures with the coupled transport and swelling and to calibrate the material models to experimental data relevant for NASA applications. Long-term, it can be applied for a range of oxidation problems in multi-layer material systems.

Acknowledgments

This project was funded by a NASA Phase II SBIR (Small Business Innovative Research) grant. Sandia National Laboratories is a multimission laboratory managed and operated by National Technology and Engineering Solutions of Sandia LLC, a wholly owned subsidiary of Honeywell International Inc. for the U.S. Department of Energy's National Nuclear Security Administration under contract DE-NA0003525.

References

[1] Piascik, B., Vickers, J., Lowry, D., Scotti, S., Stewart, J., and Calomino, A., "Materials, Structures, Mechanical Systems, and Manufacturing Roadmap-Technology Area 12," NASA Report, 2012.
[2] Luke, E.A., "A Rule-Based Specification System for Computational Fluid Dynamics," PhD. Dissertation, Mississippi State University, 1999.
[3] Timko, L.P, "Energy Efficient Engine High Pressure Turbine Component Test Performance Report," NASA Technical Reports Server, Reference Reviews, 2006.
[4] Thulin, R. D., Howe, D. C., and Singer, I. D., "Energy Efficient Engine High-Pressure Turbine Detailed Design Report," NASA Technical Reports Server, 1982.
[5] Halila, E. E., Lenahan, D. T., and Thomas, T. T., "Energy Efficient Engine High Pressure Turbine Test Hardware Detailed Design Report," NASA Technical Reports Server, 1982.
[6] Claus, R. W., Beach, T., Turner, M., and Hendricks, E. S., "Geometry and Simulation Results for a Gas Turbine Representative of the Energy Efficient Engine (EEE)," NASA Technical Reports Server, 2015.
[7] Sridhar, M., Sunnam, S., Goswami, S., and Liu, J. S., "CFD Aerodynamic Performance Validation of a Two-Stage High Pressure Turbine," *Turbo Expo: Power for Land, Sea, and Air*, Vol. 54679, Jan. 2011, pp. 1175-1184.
doi: 10.1115/GT2011-45569
[8] Silling, S. A. and Lehoucq, R. B., "Peridynamic Theory of Solid Mechanics," *Advances in Applied Mechanics,* Vol. 44, pp. 73-168, 2010.
doi: 10.1016/S0065-2156(10)44002-8
[9] http://dream3d.bluequartz.net/
[10] S. Silling, R. Cole, P. Demmie, J., Foster, and Taylor, P., "EMU User's Manual," Sandia National Laboratories, Inc., 2011.